Ultrafast time-resolved measurement of energy transport at the metal-liquid interface

Chen Chen, Iyer Vasudevan, Zhidong Du, Xianfan Xu, and Liang Pan

Citation: Appl. Phys. Lett. **112**, 253105 (2018); doi: 10.1063/1.5031875
View online: https://doi.org/10.1063/1.5031875
View Table of Contents: http://aip.scitation.org/toc/apl/112/25
Published by the American Institute of Physics

Ultrafast time-resolved measurement of energy transport at the metal-liquid interface

Chen Chen, Iyer Vasudevan, Zhidong Du, Xianfan Xu,[a] and Liang Pan[a]
School of Mechanical Engineering and Birck Nanotechnology Center, Purdue University, West Lafayette, Indiana 47907, USA

(Received 1 April 2018; accepted 11 June 2018; published online 21 June 2018)

The nanoscale light-matter interaction at metallic interfaces has many important applications, especially when it is crucial to enhance the surface-to-volume ratio and to achieve high spatial energy confinement. Here, we report an ultrafast time-resolved measurement to study photo-excited transport at the metal-liquid interfaces of colloidal gold nanoparticles (AuNPs). By using the transient absorption spectroscopy method together with the stimulated emission depletion of fluorescence molecules, we simultaneously measured the perturbations of energy states on both sides of the interfaces within a nanoscale distance. Our measurement results showed the evidence of ultrafast coupling between AuNPs and their surrounding solvent molecules at the picosecond time scale. This method can be extended to study the energy transfer mechanisms at the various interfaces for biology, chemistry, or optoelectronics. *Published by AIP Publishing.*
https://doi.org/10.1063/1.5031875

The nanoscale light-matter interaction at metallic interfaces is crucial for many nanotechnology applications. In some applications, people aim to efficiently harvest optical energy to drive physical and chemical processes near the metallic interface, such as plasmon-assisted energy conversion,[1,2] hot-electron-induced chemical reactions,[3–5] surface-enhanced Raman spectroscopy,[6] photothermal therapeutics,[7,8] drug delivery,[9] and solar thermal energy.[10,11] In other applications, people aim to minimize the light absorption and heat accumulation inside devices, such as in heat-assisted magnetic recording (HAMR),[12–14] plasmonic metamaterials, and plasmonic lithography.[15,16] Among all metallic nanoscale structures, gold nanoparticles (AuNPs) have become the subject of substantial research because of their optical, electronic and molecular-recognition properties. The light-matter interaction for AuNPs can be classically described by the two-temperature model (TTM), which characterizes energy evolutions of electron and lattice systems by electron temperature (T_e) and phonon temperature (T_p). Although some underlying physics associated with TTM are extensively studied, such as the electron-phonon interactions inside the metal and the interface transport between the lattices of the metal and the dielectric, experimental and numerical studies suggested that mechanisms for direct couplings between electrons in the metal and the lattice in the dielectric may also exist.[17–20] For AuNPs of 10 nm size and smaller, some studies discovered that significant energy dissipation may occur before the thermal equilibrium is reached between electrons and phonons inside AuNPs.[17,18] Researchers also found that different dielectric materials as surrounding matrices can lead to variations in the electron relaxation rate before the thermal equilibrium between electrons and phonons is reached inside noble metal nanoparticles and nanorods.[21–23] Some studies reported that the modifications of AuNP surface can significantly enhance the initial electron relaxation rate.[24,25] Others demonstrated direct evidence of desorption of interfacial molecules during the ultrafast optothermal process.[26–28] In our previous study, we also investigated metal-dielectric interface transport during ultrafast-laser heating of thin gold films coated on dielectric substrates,[29] which reveals the existence of a direct coupling between electrons in the metal and phonons in dielectrics which can be represented by a small contact resistance. All these studies suggested that the interface configuration can strongly affect the electron relaxation at the nanoscale. However, all of these measurements only probed the electron state at the metal side of the interface and provided no independent information about the energy state on the dielectric side of the interface.

Here, we report the simultaneous observations of energy perturbations on both sides of the metallic interface during the ultrafast optothermal transport using an experimental technique built upon the methods of ultrafast transient absorption spectroscopy (TAS).[26,30] We studied the AuNP-water system and added fluorescent molecules as indicators of energy states of solvent molecules. The solution was excited using an 800 nm pump beam with a pulse duration of about 200 fs. The short pulse duration yields a strong peak intensity that can excite the fluorescent molecules through a two-photon absorption process. The subsequent probe beam with a time delay was used to probe the transmission of AuNPs and to simultaneously perform the stimulated-emission-depletion (STED) to selectively probe the energy states of the solvent molecules within a distance of a few nanometers near the interface.

To achieve the simultaneous measurement of both TAS and the fluorescence signal, we modified a conventional pump-probe system as shown in Fig. 1(a). The TAS measurement is conducted in the transmission mode using an 800-nm excitation beam with a pulse duration of about 200 fs and a probe beam of an adjustable wavelength in the range of 500–600 nm, while the fluorescence signal is collected by another detection path orthogonal to the transmission beam

[a]Electronic addresses: xxu@purdue.edu and liangpan@purdue.edu

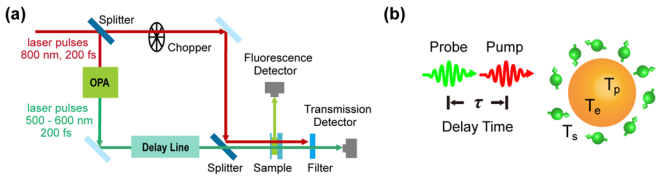

FIG. 1. Time-resolved measurement of ultrafast interface transport of gold nanoparticles (AuNPs) in fluorescence solution. (a) Experimental layout for the measurement system. (b) AuNPs surrounded by fluorescent molecules studied using the pump-probe method.

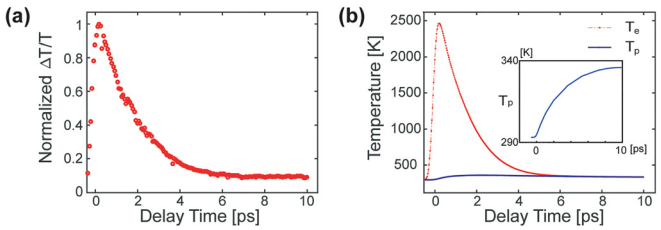

FIG. 2. Transient absorption spectroscopy (TAS) of AuNPs. (a) Normalized relative transmission change in AuNP solutions as a function of relative delay between pump and probe pulses. (b) Simulated electron and phonon temperatures. Inset: Enlarged view of photon temperature.

path. The pump and probe pulses are modulated at repetition rates of 5 kHz and 500 Hz, respectively, and the lock-in mechanism is used to enhance the signal-to-noise ratio (SNR). The pump and probe beams have a peak intensity on the order of 10^{11} W/cm^2 and 10^9 W/cm^2 at the sample,[31] respectively. The transmission of the probe pulse provides information for the electron system in AuNPs, while the perturbed fluorescent intensity provides the energy state of the liquid molecules. By varying the delay time, we can obtain the evolution of energy states of both AuNPs and surrounding solvent molecules. In our experiments, we suppressed the photobleaching effect by continuously moving the solution cuvette. The AuNP solutions (Sigma-Aldrich, stabilized suspension in citrate buffer, OD1) are used without modification. We added 10-μl 10^{-2} M fluorescein water solution into 100-μl AuNP solution. We also added 1-μl of 10 M KOH solution to increase fluorescein solubility in water.[22,26,32]

The ultrafast dynamics of 10-nm AuNPs is measured using a 520-nm probe beam, as shown in Fig. 2(a). Because of the photon energy of the probe beam is below the interband transition threshold of gold (502 nm), this TAS measurement mainly provides the thermal state of the conduction band electrons. When the pump pulse impinges on AuNPs, the free electrons inside get elevated to higher energy levels, leading to an increased transmission. The transmission reaches its peak value at the end of the pump beam. Subsequently, the AuNPs gradually relax to their original state which is captured by the probe beam as a long-tailed decay process. Figure 2(b) shows the calculated evolutions of electron and phonon temperatures inside AuNPs corresponding to the case in Fig. 2(a). As shown, the electron temperature becomes very high at the end of the pump pulse and rapidly decreases to about 1000 K after 1 ps. Meanwhile, the phonon temperature only increases by tens of Kelvins due to the large difference between the heat capacities of electrons and phonons, as shown in the inset of Fig. 2(b). At about 5 ps, the electrons and phonons mutually thermalize and reach a common temperature. The thermalized system cools slowly by dissipating its energy to the surrounding matrix. Similar to previous studies, tests on different AuNP sizes indicate that smaller particles show stronger interface coupling.[17,18]

We capture the energy states of the solvent molecules by probing the population of the excited fluorescent molecules at their lowest energy level of the excited state, as illustrated in the Franck-Condon principle diagram in Fig. 3(a). In general, stronger perturbations (i.e., more energy transfer from the AuNPs) will lead to fewer molecules at the lowest energy level of the excited state. If the evolution of population at the lowest energy level of the excited state can be obtained, we will be able to accordingly obtain the information for the energy states of the solvent molecules. This method can provide sub-ps temporal accuracy because the photo-excited molecules can reach this lowest excited state as fast as hundreds of fs through the relaxations of internal vibrational modes, in comparison to the spontaneous fluorescent emission that occurs at the nanosecond timescale. In the sub-10-ps time range, during which the ultrafast interfacial transport occurs, the response of the fluorescent molecules is dominated by the relaxation of internal vibrational modes.

The key challenge is to selectively probe the information of the solvent molecules present within a few nanometers from the metal interface. The amount of material near the interface is outweighed by that of the bulk liquid. Furthermore, photoexcited fluorescent molecules transfer a significant amount of energy to AuNPs via a non-radiative pathway. This process is referred to as fluorescence quenching and further reduces the fluorescence. In our experiments, we overcame these by enhancing the overall SNR using the plasmonic response of the AuNPs in combination with several associated effects.

The 800-nm light cannot directly excite the fluorescent molecule. Here, we used a pulse with a strong peak intensity

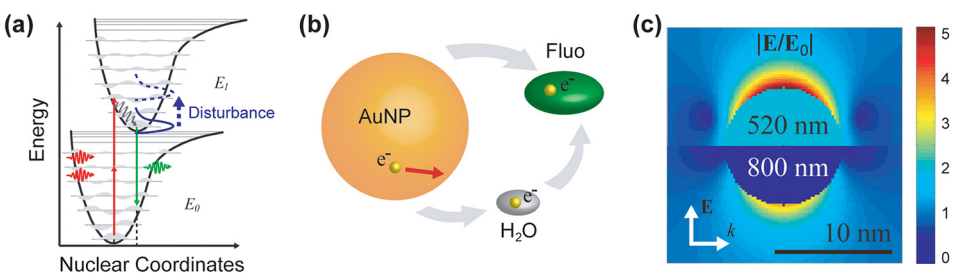

FIG. 3. Excitation of fluorescent molecules near the AuNP interface. (a) Excitation and stimulated emission depletion (STED) for fluorescent molecules in the Franck-Condon principle energy diagram. (b) Possible of coupling pathways between electrons inside AuNPs and nearby fluorescent molecules. (c) The electric field enhancement factors for a 10-nm AuNP under 520 nm and 800 nm light excitations (only one half of the image is plotted).

in the order of 10^{11} W/cm^2, which leads to two-photon excitation of fluorescent molecules. Under an 800-nm excitation, the light intensity near the surface of a 10-nm AuNP is enhanced by about 9 times [Fig. 3(c)]. This allows the strong nonlinear effect to selectively excite the fluorescent molecules near the particle surface, at a much higher probability proportional to the second order of the light intensity. The electric fields are calculated using an open-source MATLAB code implementing Mie theory.[33] After absorption, the photoexcited fluorescent molecule can be depleted by the probe beam via STED. We picked the 520-nm probe wavelength because it corresponds to the downwards transition from the lowest energy level of the excited state where we have the largest population. A higher amount of depletion corresponds to a smaller energy spread of the fluorescent molecules in the excited states, corresponding to lesser perturbation. A probe wavelength with lower photon energy will only deplete the population at higher energy levels of the excited state and therefore will not provide the desired detection sensitivity. The rate of the STED process is proportional to the intensity of depletion light. Under a 520-nm excitation, the light intensity near a 10-nm AuNP is enhanced by about 25 times [Fig. 3(c)]; therefore, the SNR of the measured STED signal is further enhanced. In addition to the two-photon and STED effects, the presence of AuNPs themselves also changes the density of states for photons which helps to boost the transition rates of nearby fluorescent molecules, known as the Purcell effect.[34,35] As an overall result, the sensitivity for the fluorescence signal near AuNPs may be significantly enhanced by orders of magnitudes.

A drawback of this detection method is the parasite optical Kerr effect,[36] wherein an undesired surge in the detected fluorescent signal is caused due to the strong excitation pulse overlapping spatially with the probe pulse inside the solution. Therefore, in the following analysis of the transmission and fluorescence signals, we only consider the portion of the captured signal with a delay longer than 800 fs, which still allows us to capture the interface transport process in the 1–10 ps time range.

Figure 4 shows the measurement results of three solutions of different particle sizes and of the same optical density at 520 nm, collected under the same pump and probe pulse fluences. The transmission measurements show the electron temperature evolution inside AuNPs. In the 1–10 ps time range, electron temperature decays almost exponentially. The magnitude of the transmission data varies for different particle sizes mainly because of the size-dependent absorptivity and the particle density in the solution. The STED signals show similar trends of exponential decays for fluorescent solutions with 10-nm and 5-nm particles but with slower decay rates. The STED signal is almost flat for the fluorescent solution containing 20-nm particles, perhaps due to their weak interface coupling. It is worthwhile to note that the STED signals for different AuNP solutions converge to a similar absolute amplitude after about 5 ps. This indicates that the fluorescent molecules reach almost the same state after several picoseconds around different sized AuNPs. When the probe wavelength changes to 536 nm, the STED signal of the 10-nm-AuNP solution shows a significantly faster decay and converges to a constant amplitude after about 2 ps. With a further increase in the probe wavelength to 555 nm, no obvious decay trend can be detected in the STED signal after an 800-fs delay.

The ultrafast interactions between the excited AuNPs and surrounding fluorescent molecules are yet to be investigated in detail. Here, we propose a possible energy pathway that may explain this coupling at the picosecond timescale. Energized electrons inside AuNPs can generate strong electromagnetic fluctuations near the particle interface and perturb the surrounding molecules. The fluorescent molecule can either directly respond to this disturbance or respond indirectly, with the disturbance being relayed by water molecules [Fig. 3(b)]. This can possibly lift the photo-excited electrons in fluorescent molecules to a higher energy level [Fig. 3(a)]. Here, we assume that the probability to lift photo-excited electrons is proportional to the energy flux from the electron system inside AuNPs. The disturbance sensed by fluorescent molecules can be estimated, as shown by the blue circles in Fig. 4(c). The fluorescent molecules have the available vibrational modes to directly couple with the energized electrons which contribute to the overall interfacial energy transport. The coupling of the disturbance directly from the AuNPs to the fluorescent molecules can be calculated using the transmission data, which is shown using a red dashed line. The water molecule relaxation process typically occurs in the ~1 ps time scale.[37] When using a 0.8-ps relaxation time for the water molecule, we found that the trend of indirect energy transfer from the disturbed water molecules to the fluorescent molecules (the black dotted line) can be well fitted to the measured STED signal (blue circles). The captured STED signal suggests that the energy transfer through water molecules could be an important energy pathway in addition to the direct coupling between the energized electrons and fluorescent molecules. It is worthwhile to point out that the measured STED signal only provides evidence of the ultrafast interface transport through

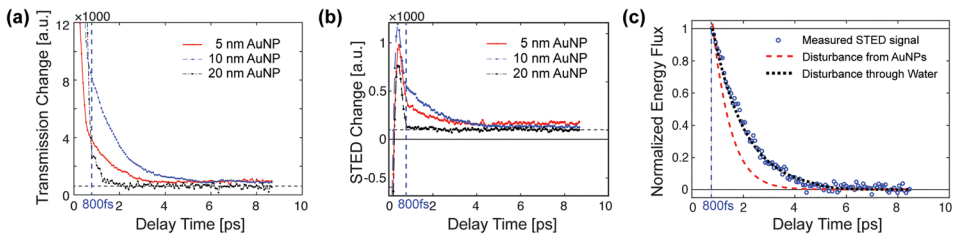

FIG. 4. Simultaneous measurements of transmission and STED signals. (a) Comparison of transient transmission signals between different sized AuNPs. (b) Comparison of the transient STED signal between different sized AuNPs at a 520-nm probe wavelength. (c) Comparison of estimated energy flux from the transmission measurement and STED measurement.

the population distribution of perturbed molecules and cannot however provide information about the average energy of the solvent molecules or the overall magnitude of the energy flux. Under such strong optothermal excitations, the energy discrepancy between the perturbed and unperturbed molecules may even preclude a well-defined average solvent temperature during the ultrafast interface transport process.

See supplementary material for more detailed descriptions of the experimental setup and comparisons of TAS measurements of water, AuNPs, and fluorescein water solutions.

This work was financially supported by the National Science Foundation (NSF) (CMMI-1405078, CMMI-1554189, and CMMI-1634832).

[1]R. K. Li, H. To, G. Andonian, J. Feng, A. Polyakov, C. M. Scoby, K. Thompson, W. Wan, H. A. Padmore, and P. Musumeci, Phys. Rev. Lett. **110**, 074801 (2013).
[2]I. Goykhman, B. Desiatov, J. Khurgin, J. Shappir, and U. Levy, Nano Lett. **11**, 2219 (2011).
[3]S. Mukherjee, F. Libisch, N. Large, O. Neumann, L. V. Brown, J. Cheng, J. B. Lassiter, E. A. Carter, P. Nordlander, and N. J. Halas, Nano Lett. **13**, 240 (2013).
[4]S. Mubeen, J. Lee, N. Singh, S. Kramer, G. D. Stucky, and M. Moskovits, Nat. Nanotechnol. **8**, 247 (2013).
[5]P. Christopher, H. Xin, A. Marimuthu, and S. Linic, Nat. Mater. **11**, 1044 (2012).
[6]M. Moskovits, Rev. Mod. Phys. **57**, 783 (1985).
[7]V. P. Zharov, K. E. Mercer, E. N. Galitovskaya, and M. S. Smeltzer, Biophys. J. **90**, 619 (2006).
[8]S. Wang, A. Riedinger, H. Li, C. Fu, H. Liu, L. Li, T. Liu, L. Tan, M. J. Barthel, G. Pugliese, F. De Donato, M. Scotto D'Abbusco, X. Meng, L. Manna, H. Meng, and T. Pellegrino, ACS Nano **9**, 1788 (2015).
[9]S. Purushotham, P. E. J. Chang, H. Rumpel, I. H. C. Kee, R. T. H. Ng, P. K. H. Chow, C. K. Tan, and R. V. Ramanujan, Nanotechnology **20**, 305101 (2009).
[10]S. Chen and S. Z. Qiao, ACS Nano **7**, 10190 (2013).
[11]O. Neumann, A. S. Urban, J. Day, S. Lal, P. Nordlander, and N. J. Halas, ACS Nano **7**, 42 (2013).
[12]N. J. Gokemeijer, W. A. Challener, E. Gage, Y. T. Hsia, G. Ju, D. Karns, L. Li, B. Lu, K. Pelhos, C. Peng, T. Rausch, R. E. Rottmayer, M. A. Seigler, X. Yang, and H. Zhou, J. Magn. Soc. Jpn. **32**, 146 (2008).
[13]L. Pan and D. B. Bogy, Nat. Photonics **3**, 189 (2009).
[14]W. A. Challener, C. B. Peng, A. V. Itagi, D. Karns, W. Peng, Y. Y. Peng, X. M. Yang, X. B. Zhu, N. J. Gokemeijer, Y. T. Hsia, G. Ju, R. E. Rottmayer, M. A. Seigler, and E. C. Gage, Nat. Photonics **3**, 220 (2009).
[15]W. Srituravanich, L. Pan, Y. Wang, C. Sun, D. B. Bogy, and X. Zhang, Nat. Nanotechnol. **3**, 733 (2008).
[16]L. Pan, Y. Park, Y. Xiong, E. Ulin-Avila, Y. Wang, L. Zeng, S. Xiong, J. Rho, C. Sun, D. B. Bogy, and X. Zhang, Sci. Rep. **1**, 175 (2011).
[17]M. Hu and G. V. Hartland, J. Phys. Chem. B **106**, 7029 (2002).
[18]G. V. Hartland, Chem. Rev. **111**, 3858 (2011).
[19]Z. Lu, Y. Wang, and X. Ruan, Phys. Rev. B **93**, 064302 (2016).
[20]D. Jin, Q. Hu, D. Neuhauser, F. von Cube, Y. Yang, R. Sachan, T. S. Luk, D. C. Bell, and N. X. Fang, Phys. Rev. Lett. **115**, 193901 (2015).
[21]V. Halté, J. Y. Bigot, B. Palpant, M. Broyer, B. Prével, and A. Pérez, Appl. Phys. Lett. **75**, 3799 (1999).
[22]S. Link, D. J. Hathcock, B. Nikoobakht, and M. A. El-Sayed, Adv. Mater. **15**, 393 (2003).
[23]M. B. Mohamed, T. S. Ahmadi, S. Link, M. Braun, and M. A. El-Sayed, Chem. Phys. Lett. **343**, 55 (2001).
[24]S. L. Westcott, R. D. Averitt, J. A. Wolfgang, P. Nordlander, and N. J. Halas, J. Phys. Chem. B **105**, 9913 (2001).
[25]K. O. Aruda, M. Tagliazucchi, C. M. Sweeney, D. C. Hannah, G. C. Schatz, and E. A. Weiss, Proc. Natl. Acad. Sci. U.S.A. **110**, 4212 (2013).
[26]X. Wu, Y. Ni, J. Zhu, N. D. Burrows, C. J. Murphy, T. Dumitrica, and X. Wang, ACS Appl. Mater. Interfaces **8**, 10581 (2016).
[27]P. K. Jain, W. Qian, and M. A. El-Sayed, J. Am. Chem. Soc. **128**, 2426 (2006).
[28]A. J. Schmidt, J. D. Alper, M. Chiesa, G. Chen, S. K. Das, and K. Hamad-Schifferli, J. Phys. Chem. C **112**, 13320 (2008).
[29]L. Guo, S. L. Hodson, T. S. Fisher, and X. Xu, J. Heat Transfer **134**, 042402 (2012).
[30]J. Huang, J. Park, W. Wang, C. J. Murphy, and D. G. Cahill, ACS Nano **7**, 589 (2013).
[31]M. Rasmusson, A. N. Tarnovsky, E. Åkesson, and V. Sundström, Chem. Phys. Lett. **335**, 201 (2001).
[32]S. C. Nguyen, Q. Zhang, K. Manthiram, X. Ye, J. P. Lomont, C. B. Harris, H. Weller, and A. P. Alivisatos, ACS Nano **10**, 2144 (2016).
[33]J. P. Schäfer, Ph.D. dissertation, Universität Ulm, 2011.
[34]S. Sun, L. Wu, P. Bai, and C. E. Png, Phys. Chem. Chem. Phys. **18**, 19324 (2016).
[35]P. Anger, P. Bharadwaj, and L. Novotny, Phys. Rev. Lett. **96**, 113002 (2006).
[36]S. Palese, L. Schilling, R. J. D. Miller, P. R. Staver, and W. T. Lotshaw, J. Phys. Chem. A **98**, 6308 (1994).
[37]H. K. Nienhuys, S. Woutersen, R. A. v. Santen, and H. J. Bakker, J. Chem. Phys. **111**, 1494 (1999).